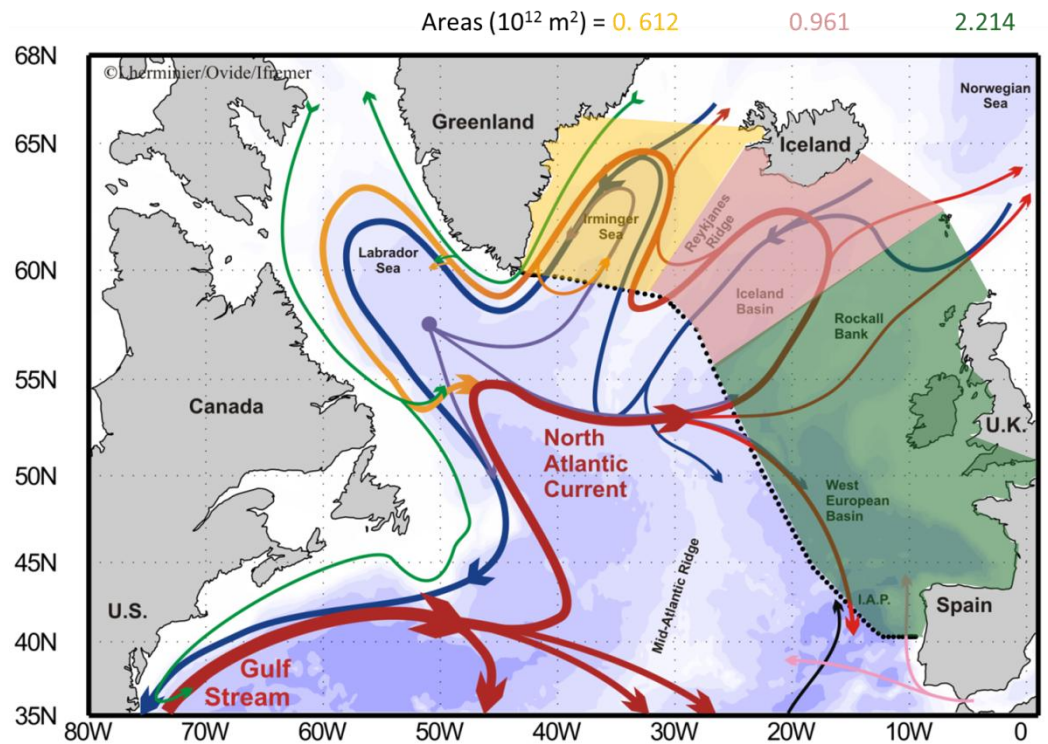


Patricia ZUNINO<sup>1</sup>  
 Fiz F. PEREZ<sup>2</sup>  
 Pascale LHERMINIER<sup>1</sup>  
 Herlé MERCIER<sup>1</sup>

Juin 2015 – LPO/15-03

## Computing inventories of anthropogenic CO<sub>2</sub> in the eastern subpolar North Atlantic using OVIDE data



# **Computing inventories of anthropogenic CO<sub>2</sub> in the eastern subpolar North Atlantic using OVIDE data**

**Improvement of the methodology developed by Pérez et al. (2010)**

---

## CONTENTS

1. Introduction.....	5
2. Computing $C_{ant}$ inventories step by step .....	6
2.1. Data.....	6
2.2. Methods.....	6
3. Error computation.....	11
4. Differences between $C_{ant}$ inventories estimated by Pérez et al. (2010) method and by the improved method.....	11
5. Conclusions .....	13

---

## ABSTRACT

The highest anthropogenic CO<sub>2</sub> (C<sub>ant</sub>) inventories of all the oceans are found in the subpolar North Atlantic (SPNA). The OVIDE section crosses the SPNA from Greenland to Portugal and is repeated biennially since 2002. Therefore, OVIDE data allow evaluating the evolution of inventories of anthropogenic CO<sub>2</sub> (C<sub>ant</sub>) in the SPNA. This oceanic region is known to host water formation and ventilation processes that change the water mass volumetric census year by year. Changes in the volumetric census cause differences in the C<sub>ant</sub> inventory estimates (Pérez et al., 2008). Consequently, Pérez et al. (2010) proposed a method for computing C<sub>ant</sub> inventory in the SPNA taking into account the volumetric census variability and a bathymetric adjustment. This method has been recently revised. The initial methodology and the recent improvements are detailed in this report.

## 1. Introduction

The ocean plays an important role in the actual climate change scenarios. One of the reasons is that it uptakes part of the CO<sub>2</sub> emitted by human activities from the atmosphere. Since the beginning of the industrial revolution, a third of the total CO<sub>2</sub> emitted by human activities ( $C_{\text{ant}}$  hereafter) has been absorbed by the ocean (Kathiwala et al., 2013). However,  $C_{\text{ant}}$  is not equally accumulated in all the oceans: the highest  $C_{\text{ant}}$  storage rates are found in the subpolar North Atlantic (Sabine et al., 2004; Kathiwala et al., 2013).

The OVIDE section (<http://wwz.ifremer.fr/lpo/La-recherche/Projets-en-cours/OVIDE>) crosses the subpolar North Atlantic (SPNA) from Greenland to Portugal. It is repeated biennially since 2002. Physical and biogeochemical parameters are measured from surface to bottom at about 90 hydrographic stations along this section. Some of the measured biogeochemical properties are total CO<sub>2</sub> ( $C_T$ ), total alkalinity ( $A_T$ ), pH, oxygen and nutrients.  $C_{\text{ant}}$  concentration in the water can be estimated using some of these properties together with temperature, salinity and the air-sea disequilibrium of CO<sub>2</sub> by applying the  $\phi C_t^\circ$  method (Vazquez et al., 2009). Therefore, OVIDE data provide an important tool to quantify  $C_{\text{ant}}$  inventories in the SPNA, to evaluate its interannual variability and, soon, its long term variability.

Previous works estimated  $C_{\text{ant}}$  storage rates in different areas of the North Atlantic applying the mean penetration depth (MPD) method and using data from a single cruise (e.g. Alvarez et al., 2003; Rosón et al., 2003). This method assumes that MPD is constant in time. However, MPD is not constant in areas where ventilation and/or water formation processes occur and the variability of the MPD could notoriously affects the estimates of  $C_{\text{ant}}$  storage rates (Pérez et al., 2008). The SPNA is an area where ventilation and/or water formation processes take place (Yashayaev et al., 2007; Vage et al., 2009; among others): consequently, the MPD method is not appropriate to estimate  $C_{\text{ant}}$  storage rates in this region. Pérez et al. (2010) proposed a method for quantifying  $C_{\text{ant}}$  inventories in the SPNA using cruise data and taking into account changes in the water mass volumetric census. The method has been recently revised. The details of Pérez et al. (2010) method and the recent improvements are detailed in this report.

## 2. Computing $C_{ant}$ inventories step by step

### 2.1. Data

The  $C_{ant}$  concentration in a water sample can be estimated from other biogeochemical properties using back-calculation or tracer-based methods. In our case,  $C_{ant}$  is estimated from  $C_T$ ,  $A_T$ , oxygen, temperature, salinity and nutrients using  $\phi Ct^\circ$  method (Vazquez et al., 2009). For details about the sampling and methods used for measuring each property the reader is referred to García-Ibáñez (2015). The above properties, except temperature and salinity that are measured continuously by the CTD, are measured at 24 discrete depths where Niskin bottles were closed; consequently,  $C_{ant}$  concentrations are estimated at discrete depths. Later, at each station,  $C_{ant}$  estimates are vertically linearly interpolated every meter.

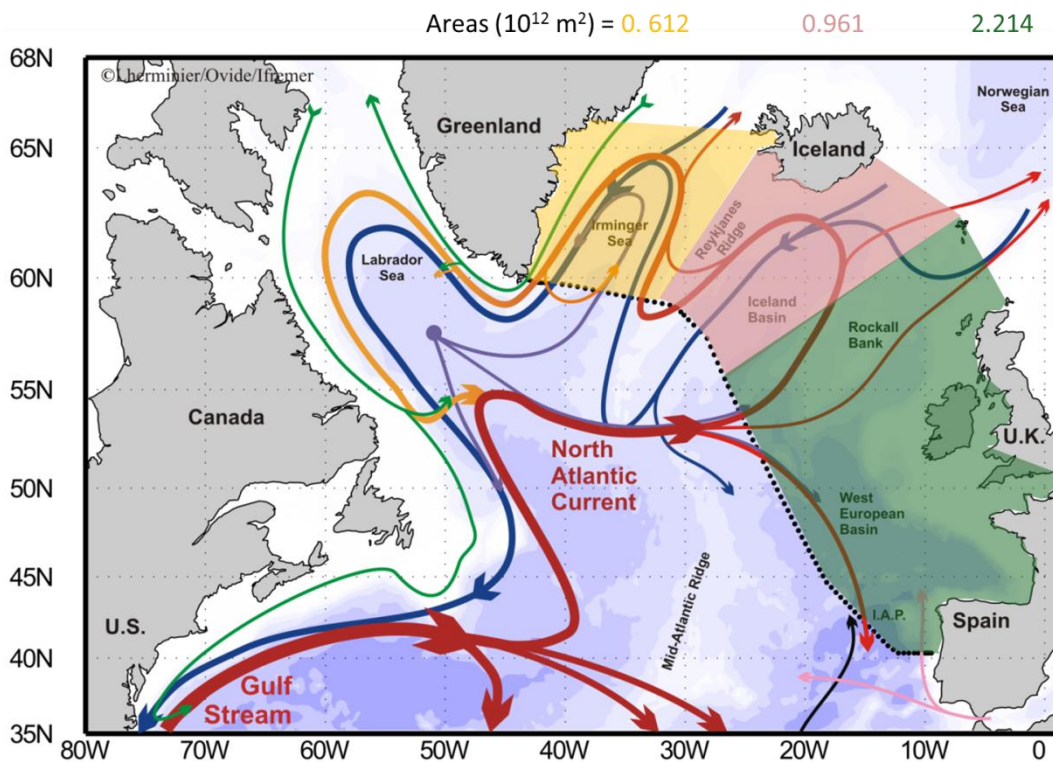


Figure 1: Schematic circulation in the North Atlantic. Dotted line indicates the location of the OVIDE section. Shaded areas are the three region we have divided the eastern-SPNA: the Irminger Sea in yellow ( $0.612 \cdot 10^{12} \text{ km}^2$ ), the Iceland Basin in pink ( $0.961 \cdot 10^{12} \text{ km}^2$ ) and the Eastern North Atlantic in green ( $2.214 \cdot 10^{12} \text{ km}^2$ ).

### 2.2. Methods

The method is developed to compute  $C_{ant}$  inventories in the waters confined between the OVIDE section and the Greenland-Iceland-Scotland (G-I-S) sills. This region, eastern-SPNA hereafter, has a total surface of  $3.787 \cdot 10^{12} \text{ m}^2$  (Figure 1). The  $C_{ant}$  inventories are directly proportional to the water volume. Following Pérez et al. (2010), the  $C_{ant}$  inventories are

computed in each water mass as defined in table 1 using data from the OVIDE section. The volume of each water mass depends on the bathymetry of the whole area – which is not exactly the same than at the section (OVIDE) – and on the water mass volumetric census that can change year by year in this region due to ventilation processes (Pérez et al., 2008). In order to deal with the bathymetry of the whole section, a bathymetric adjustment is applied, that will be explained hereafter. Concerning the volumetric census, the eastern-SPNA does not present the same dynamics everywhere: changes in the volumetric census of water masses affect the Irminger Sea and Iceland Basin, however they are negligible in the Eastern North Atlantic (ENA, see Fig. 1) because its remoteness from deep convection sites. Therefore, the eastern-SPNA is divided into three basins (Irminger Sea, Iceland Basin and Eastern North Atlantic, see Fig. 1) and two different methods for computing  $C_{ant}$  inventories are proposed to take into account those geographical specificities.

Method 1: applicable for computing  $C_{ant}$  inventories in the ENA Basin. It takes into account only bathymetry adjustment. The  $C_{ant}$  inventory ( $Inv$ ) in the ENA basin using data of a single cruise (c) is computed as the sum of  $C_{ant}$  inventory in each water mass (w) following equation 1:

$$Inv_{ENA,c} = \sum_{w=1}^k (Th_{w,ENA}^{WOA} \cdot \rho_{w,ENA,c} \cdot [C_{ant}]_{w,ENA,c} \cdot Th_{w,ENA}^{WOA}) \quad (1)$$

where  $k$  is the total number of water masses;  $\rho_{w,ENA,c}$  and  $[C_{ant}]_{w,ENA,c}$  stand for the mean values of *in situ* density and  $C_{ant}$  concentration, respectively, of each water mass in the ENA basin;  $Th_{w,ENA}^{WOA}$  is the climatological thickness of each water mass (w) in the ENA basin. For computing  $\rho_{w,ENA,c}$  and  $[C_{ant}]_{w,ENA,c}$ , the depth range of the water mass is previously determined (water mass limits defined in table 1) at each cruise station and a mean value of both properties is computed for the corresponding layer. At this point, the Pérez et al. (2010) methodology is slightly improved: while in Pérez et al. (2010) the  $[C_{ant}]_{w,b,c}$  was computed averaging the bottle values following the trapezoid rule in both vertical and horizontal dimensions, the bottle data are now linearly interpolated every meter before obtaining a mean value for the water mass layer. The vertical interpolation also improves the determination of water mass depth range; indeed, in Pérez et al. (2010) method, the depth of an isopycnal defining the limit between two water masses was determined at the half-distance between two consecutive bottle samples located in two different water masses. Once  $[C_{ant}]$  and  $\rho$  are determined for each water mass at each cruise station,  $\rho_{w,ENA,c}$  and  $[C_{ant}]_{w,ENA,c}$  are finally computed as the mean value of all the stations in the ENA basin.

Table 1: Water masses description in each basin. Density limits have been defined following Kieke et al., (2007), Yashayaev et al. (2008) and Pérez et al. (2010).  $Th_{w,b}^{WOA05}$  is the climatological water mass thicknesses computed as the ratio between the total volume of each water in each basin obtained from WOA05 data and the surface area of each basin.

ENA			ICELAND BASIN			IRMINGER SEA		
Area=2.214 10 <sup>12</sup> m <sup>2</sup>			Area=0.961 10 <sup>12</sup> m <sup>2</sup>			Area=0.612 10 <sup>12</sup> m <sup>2</sup>		
Volume= 5.38 10 <sup>15</sup> m <sup>3</sup>			Volume= 1.60 10 <sup>15</sup> m <sup>3</sup>			Volume= 0.96 10 <sup>15</sup> m <sup>3</sup>		
Water mass	Density limits (kg m <sup>-3</sup> )	$Th_{w,b}^{WOA05}$ (m)	Water mass	Density limits (kg m <sup>-3</sup> )	$Th_{w,b}^{WOA05}$ (m)	Water mass	Density limits (kg m <sup>-3</sup> )	$Th_{w,b}^{WOA05}$ (m)
NACW	$\sigma_0 < 27.20$	256	SAIW	$\sigma_0 < 27.60$	636	SAIW	$\sigma_0 < 27.68$	434
MW	$\sigma_0 > 27.20$ ; $\sigma_1 < 32.35$	791	uLSW	$\sigma_0 > 27.60$ ; $\sigma_1 < 32.35$	360	uLSW	$27.68 < \sigma_0 < 27.76$	358
LSW	$\sigma_1 > 32.35$ ; $\sigma_2 < 37.00$	511	cLSW	$\sigma_1 > 32.35$ ; $\sigma_2 < 37.00$	529	cLSW	$27.76 < \sigma_0 < 27.81$	453
uNADW	$\sigma_2 < 37.00$ ; $\sigma_4 < 45.84$	549	uNADW	$\sigma_2 < 37.00$ ; $\sigma_4 < 45.84$	149	uNADW	$27.81 < \sigma_0 < 27.88$	275
INADW	$\sigma_4 > 45.84$	321				DSOW	$\sigma_0 > 27.88$	56

The  $Th_{w,ENA}^{WOA}$  is used in order to apply the bathymetric adjustment since the bathymetric along the cruise section is not exactly the same for the whole basin. It is computed using the World Ocean Atlas 2005 climatology (WOA05; <http://www.nodc.noaa.gov/OC5/WOA05/woa05data.html>). The volume of each water mass are estimated for every WOA05 grid point (1° latitude x 1° longitude resolution), after determining the position of the water masses in the water column using the potential density intervals in Table 1. The total volume of each water mass in the basin is the integration over all grid points inside the basin. The climatological volumes are converted to climatological thicknesses ( $Th_{w,ENA}^{WOA05}$ , see table 1) considering the ENA basin surface area (2.214 x 10<sup>12</sup> m<sup>2</sup>). The bathymetric adjustment allows the Cant inventory, in mol C m<sup>-2</sup>, computed from OVIDE data to be representative of the whole ENA basin.

Because the ENA basin accounts for a large area, the Cant concentration measured at the OVIDE section may not be spatially homogeneous in each water mass over the whole basin. We have evaluated the spatial correction proposed by Pérez et al. (2010) based on a



Multilinear Regression (MLR) fit of the anomalies of AOU, temperature and salinity from different cruises. We find that the MLR coefficients depend too much on the considered datasets; furthermore, the resulting  $C_{ant}$  inventory is not significantly changed by this correction. Consequently, we decided not to apply the  $C_{ant}$  concentration correction in the ENA basin.

Method 2: applicable for computing  $C_{ant}$  inventories in the Irminger Sea and Iceland Basin. It takes into account changes in the volumetric census of water masses and the bathymetry of the whole basin. The  $C_{ant}$  inventory ( $Inv$ ) in the basin (b) using data of a single cruise (c) is computed as the sum of  $C_{ant}$  inventory in each water mass (w) following equation 2:

$$Inv_{b,c} = \sum_{w=1}^k (\rho_{w,b,c} \cdot [C_{ant}]_{w,b,c} \cdot Th_{w,b,c}^*) \quad (2)$$

where  $k$  is the total number of water masses;  $\rho_{w,b,c}$  and  $[C_{ant}]_{w,b,c}$  stand for the mean values of *in situ* density and  $C_{ant}$  concentration, respectively, of each water mass (w) in the basin (b) and cruise (c);  $Th_{w,b,c}^*$  is the vertical thickness of each water mass (w) in the basin (b) and cruise (c), after correction of both the volumetric census variability and the bathymetry of the whole basin. The only different between equation 1 and 2 is the thickness term, while in equation 1 a climatological thickness is used, in equation 2 the thickness term also includes an adjustment accounting for the changes in the volumetric census of the water masses in the Iceland Basin and Irminger Sea.

The volumetric census is corrected by factor  $F_{w,b,c}$ . This factor is computed as the ratio of the normalized thickness of each water mass using the cruise data and the WOA05 data (equation 3). Specifically, at each cruise station, water mass thicknesses are computed with both cruise data ( $Th_{w,b,c}^{obs}$ ) and WOA05 data ( $Th_{w,b,c}^{WOA05}$ ). Water mass thicknesses using WOA05 data are computed as follows. First, potential densities ( $\sigma_0, \sigma_1, \sigma_2, \sigma_4$ ) are computed at each WOA05 grid point and then interpolated in latitude, longitude and pressure at the position of each cruise profile; note that the maximal depth of the interpolated WOA05 data profile is adjusted to the measured depth at the OVIDE station. Second, the thickness of each water mass at each cruise station is computed using the WOA05 3-dimensionally interpolated data. Then, the thickness mean values ( $Th_{w,b,c}^{WOA05}$ ) for each water mass (w) and basin (b) is estimated by averaging the thicknesses estimated at the stations of each cruise (c). Finally,  $F_{w,b,c}$  is obtained by dividing the normalized  $Th_{w,b,c}^{obs}$  and  $Th_{w,b,c}^{WOA05}$  as exposed in equation 3, where  $k$  is the total number of water masses:

$$F_{w,b,c} = \frac{Th_{w,b,c}^{obs} / \sum_{w=1}^k Th_{w,b,c}^{obs}}{Th_{w,b,c}^{WOA05} / \sum_{w=1}^k Th_{w,b,c}^{WOA05}} \quad (3)$$

The 3-dimensionally interpolation of WOA05 data from their grid points to the real station position and the fitting of maximal depth of the WOA05 profiles to those measured at the real station are light improvements of the Pérez et al. (2010) method; indeed, they simply used the data of the nearest WOA05 grid point to the real station without spatial interpolation.

The following step is the bathymetric correction, since the bottom ocean is not flat and the OVIDE section bathymetry is not exactly the same than those of the whole east-SPNA. Therefore, the climatological thickness of each water mass,  $Th_{w,b}^{WOA05}$  is estimated for the Iceland Basin and Irminger sea in the same way  $Th_{w,ENA}^{WOA05}$  was computed (explained in the method 1). All climatological thicknesses are included in Table 1. Note that  $Th_{w,b}^{WOA05}$  and  $Th_{w,b,c}^{WOA05}$  are different:  $Th_{w,b}^{WOA05}$  is the climatological thickness of each water mass representative of the basin, and  $Th_{w,b,c}^{WOA05}$  is the mean value of the water mass thicknesses computed at each cruise station using the interpolated WOA05 data.

The water mass thickness computed from cruise data, with volume census variability and bathymetric correction is computed as:

$$Th'_{w,b,c} = Th_{w,b}^{WOA05} \cdot F_{w,b,c} \quad (4)$$

Additionally, like in Pérez et al. (2010), we find another caveat in the computation of the water mass thicknesses representative of the Iceland Basin and Irminger basin: the methodology does not assure  $\sum_{w=1}^k Th'_{w,b,c} = \sum_{w=1}^k Th_{w,b}^{WOA05}$ . Therefore a standardization factor ( $f_{b,c}$ ) is still necessary in order to assure that  $\sum_{w=1}^k Th'_{w,b,c} = \sum_{w=1}^k Th_{w,b}^{WOA05}$ . This factor is computed as:

$$f_{b,c} = \sum_{w=1}^k Th'_{w,b,c} / \sum_{w=1}^k Th_{w,b}^{WOA05} \quad (5)$$

which is very close to 1. Finally, the water mass thicknesses, with volumetric census variability and bathymetric adjustment, to be used in equation 2 are computed as:

$$Th_{w,b,c}^* = Th'_{w,b,c} \cdot \frac{1}{f_{b,c}} \quad (6)$$

The improvement of Pérez et al. (2010) method is mainly reflected in the method 2, although method 1 is also affected in the vertical interpolation of bottle data. The improvements of the Pérez et al. (2010) can be summarized as:

1. The  $C_{ant}$  concentrations estimated from each bottle sample taken at the OVIDE stations are vertically interpolated each meter before computing the mean  $C_{ant}$  value for each water mass.

2. The density fields computed at WOA05 grid points are 3-dimensionally interpolated to each OVIDE station.
3. For the computation and comparison of water mass thicknesses at each station (OVIDE vs WOA05 interpolated data), the bottom depth is homogenized.

Once  $C_{\text{ant}}$  inventories are estimated in Irminger Sea, Iceland Basin and ENA applying the appropriate method, the eastern-SPNA  $C_{\text{ant}}$  inventory is estimated as the area weighted average of the inventories in each basin.

The method has been exposed for computing  $C_{\text{ant}}$  inventories. However, it can also be applied for the computation of dissolved inorganic carbon (DIC) inventories, changing  $[C_{\text{ant}}]$  to  $[\text{DIC}]$  in the previous equations, with  $[\text{DIC}]$  being the DIC concentration in  $\mu\text{mol kg}^{-1}$ .

### 3. Error computation

The errors of  $C_{\text{ant}}$  and DIC inventories depend on the analytical errors ( $5.2 \mu\text{mol kg}^{-1}$  and  $4 \mu\text{mol kg}^{-1}$  for  $C_{\text{ant}}$  and DIC respectively) and on the time and the space variability of  $C_{\text{ant}}$  and DIC caused by internal waves and mesoscale activity. In order to take into account these errors we adopt a specific procedure. The error is estimated as the standard deviation of the  $C_{\text{ant}}$  and DIC inventories computed 100 times from the original data randomly perturbed within twice the analytical errors, e.g.  $10.4 \mu\text{mol kg}^{-1}$  and  $8 \mu\text{mol kg}^{-1}$  for  $C_{\text{ant}}$  and DIC respectively. The errors of  $C_{\text{ant}}$  and DIC inventories in the eastern-SPNA box are  $0.57$  and  $0.47 \text{ mol C m}^{-2} \text{ yr}^{-1}$ , respectively. However, there is an additional error related to the extrapolation of the cruise data to the whole basin. In Pérez et al. (2010),  $C_{\text{ant}}$  inventories in the eastern-SPNA were computed using all the available cruise dataset within the eastern-SPNA from 1981 to 2006. They found a difference of  $2 \text{ mol C m}^{-2}$  in the  $C_{\text{ant}}$  inventory depending on the position of the cruise stations (see their figure 3). This error, larger than those due to the internal activity of the ocean, is considered as the error of our estimates of  $C_{\text{ant}}$  and DIC inventories.

### 4. Differences between $C_{\text{ant}}$ inventories estimated by Pérez et al. (2010) method and by the improved method

Figure 2 displays  $C_{\text{ant}}$  inventories from 2002 to 2010 estimated by both, Pérez et al. (2010) method and the improved method. Some differences in the  $C_{\text{ant}}$  inventories estimated by both

methods are found in the Irminger Sea and Iceland Basin, yet they are not statistically different considering the associated errors.

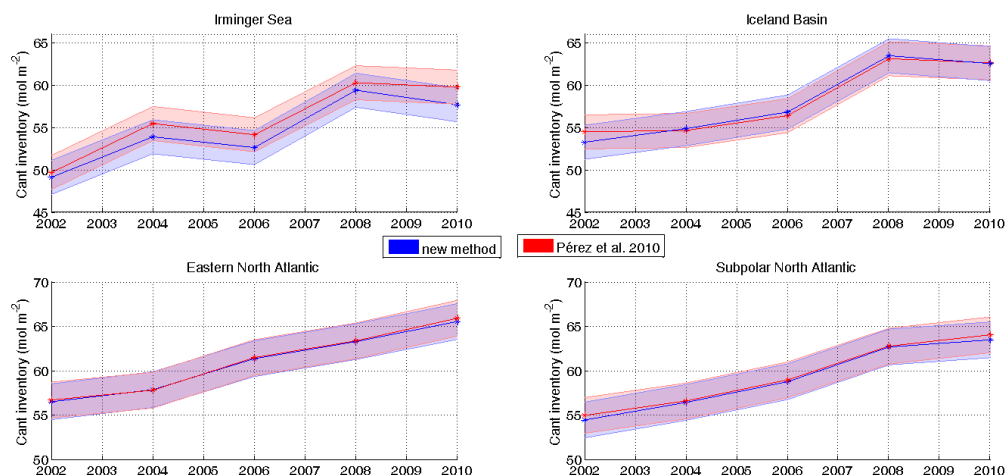


Figure 2. Time evolution (2002-2010) of  $C_{ant}$  inventories estimated by both the Pérez et al. (2010) method (red) and the improved method (blue) in the Irminger Sea, Iceland Basin, Eastern North Atlantic and the eastern subpolar North Atlantic.

The  $C_{ant}$  storage rates are computed from  $C_{ant}$  inventory time series. Table 2 shows  $C_{ant}$  storage rates computed from both inventory time series. Again, some differences are found in the results obtained for the Irminger Sea and the Iceland Basin, yet, they are not statistically different.

Table 2.  $C_{ant}$  storage rates estimated at each basin and for the whole eastern Subpolar North Atlantic from the inventory time series obtained by the Pérez et al. (2010) method and by the improved method.

Unit: $\text{mol C m}^{-2} \text{ yr}^{-1}$	Pérez et al. (2010) method	Improved method
Irminger Sea	$1.25 \pm 0.34$	$1.13 \pm 0.36$
Iceland Basin	$1.23 \pm 0.33$	$1.35 \pm 0.29$
ENA	$1.19 \pm 0.10$	$1.17 \pm 0.08$
SPNA	$1.21 \pm 0.11$	$1.21 \pm 0.12$

## 5. Conclusions

The Pérez et al. (2010) method for computing  $C_{\text{ant}}$  inventories has been improved. The improvements are: (i) the  $C_{\text{ant}}$  concentration estimated from bottle samples are vertically interpolated each meter before obtaining  $C_{\text{ant}}$  mean values for each water mass; (ii) WOA05 data are 3-dimensionally interpolated to the position of the OVIDE stations to determine the volumetric census correction, and each pair of profiles to be compared (OVIDE and WOA05) have the same maximal depth.

The light modifications in the method do not cause differences statistically significant neither in the estimations of  $C_{\text{ant}}$  inventories nor in the computation of  $C_{\text{ant}}$  storage rates. Nevertheless, we consider the improvements are necessary to obtain more reliable estimates of  $C_{\text{ant}}$  inventories and  $C_{\text{ant}}$  storage rates at long term. This report is a guide for computing  $C_{\text{ant}}$  and DIC inventories in the eastern-SPNA using OVIDE data. This improved method was used in Zunino et al. (submitted to GRL).

## References

Álvarez, M., Rios, A.F., Pérez, F.F., Bryden, H.L., Roson, G.: Transports and budgets of total inorganic carbon in the Subpolar and Temperate North Atlantic, *Global Biogeochem Cy*, 17(1), 1002, doi:10.1029/2002GB001881, 2003.

García-Ibáñez, M. I., Acidification and transports of water masses and  $\text{CO}_2$  in the North Atlantic, PhD Thesis.

Khatiwala, S., Tanhua T., Mikaloff Fletcher S., Gerber M., Doney S.C., Graven H. D., Gruber N., McKinley G.A., Murata A., Rios A.F. and Sabine C.L.: Global ocean storage of anthropogenic carbon. *Biogeosciences*, 10, 2169-2191, doi: 10.5194/bg-10-2169-2013, 2013.

Kieke, D., Rhein, M., Stramma, L., Smethie, W. M., Bullister, J. L., and LeBel, D. A.: Changes in the pool of Labrador Sea Water in the subpolar North Atlantic, *Geophys. Res. Lett.*, 34, L06605, doi:10.1029/2006GL028959, 2007.

Pérez, F. F., Vázquez-Rodríguez, M., Louarn, E., Padn, X. A., Mercier, H., and Rios, A. F.: Temporal variability of the anthropogenic  $\text{CO}_2$  storage in the Irminger Sea, *Biogeosciences*, 5, 1669–1679, doi:10.5194/bg-5-1669-2008, 2008.

Pérez, F.F., Vazquez-Rodriguez M., Mercier H., Velo A., Lherminier P. and Rios A. F.: Trends of anthropogenic  $\text{CO}_2$  storage in North Atlantic water Masses, *Biogeosciences*, 7, 1789–1807, doi:10.5194/bg-7-1789-2010, 2010.

Roson, G., Rios, A.F., Lavin, A., Bryden, H.L., Pérez, F.F.: Carbon distribution, fluxes and budgets in the subtropical North Atlantic, *J Geophys Res*, 108, doi:10.1029/1999JC000047, 2003.

Sabine, C. L., Feely, R. A., Gruber, N., Key, R. M., Lee, K., Bullister, J. L., Wanninkhof, R., Wong, C. S., Wallace, D. W. R., Tilbrook, B., Millero, F. J., Peng T.-H., Kozyr, A., Ono, T., and Rios, A. F.: The oceanic sink for anthropogenic  $\text{CO}_2$ , *Science*, 305, 367–371, 2004. Yashayaev, I., Holliday, N. P., Bersch, M., and van Aken, H. M.: The history

---

of the Labrador Sea Water: Production, Spreading, Transformation and Loss. In “Arctic-Subarctic Ocean Fluxes: defining the role of the Northern Seas in climate”, edited by: Robert, R., Dickson, J., and Meincke, P., Rhines. Springer, P.O. Box 17, 3300 AA Dordrecht, The Netherlands, pp. 569– 612, 2008.

Våge K., R. Pickart, V. Thierry, G. Reverdin, C. Lee, B. Petrie, T. Agnew, A. Wong and M. H. Ribergaard, 2009. Surprising return of deep convection to the subpolar North Atlantic Ocean in winter 2007–2008. *Nature Geoscience*. doi: 10.1038/NGEO382

Vázquez-Rodríguez, M., Padin, X. A., Ríos, A. F., Bellerby, R. G. J., and Pérez, F. F.: An upgraded carbon-based method to estimate the anthropogenic fraction of dissolved CO<sub>2</sub> in the Atlantic Ocean, *Biogeosciences Discuss.*, 6, 4527–4571, doi:10.5194/bgd-6-4527-2009, 2009.

Yashayaev, I., H. M. van Aken, N. P. Holliday, and M. Bersch (2007), Transformation of the Labrador Sea Water in the subpolar North Atlantic, *Geophys. Res. Lett.*, 34, L22605, doi:10.1029/2007GL031812.